

Self-extinguishing polymer/organoclay nanocomposites

Mayu Si^a, Vladimir Zaitsev^a, Michael Goldman^b, Anatoly Frenkel^c, Dennis G. Peiffer^d,
Edward Weil^e, Jonathan C. Sokolov^a, Miriam H. Rafailovich^{a,*}

^a Department of Materials Science and Engineering, State University of New York at Stony Brook, Stony Brook, NY 11794-2275, USA

^b Yeshiva College, Yeshiva University, New York, NY 10016, USA

^c Physics Department, Yeshiva University, New York, NY 10016, USA

^d ExxonMobil Research and Engineering Company, Annandale, NJ 08801, USA

^e Polymer Research Institute, Polytechnic University, Brooklyn, NY 11201, USA

Received 14 May 2006; received in revised form 10 August 2006; accepted 15 August 2006

Available online 30 October 2006

Abstract

We demonstrated that self-extinguishing polymer nanocomposites, which can pass the stringent UL 94 V0 standard, can be successfully prepared by combining modified organoclays with traditional flame retardant (FR) agents. Using secondary ion mass spectrometry (SIMS) and transmission electron microscopy (TEM), we determined that the addition of modified clays, which can intercalate or exfoliate in the matrix, also improved the dispersion of the FR agents. Dynamic mechanical analysis (DMA) indicated that the clays increased the modulus of the polymer above T_g , which prevented dripping during burning. Cone calorimetry test showed that the nanocomposites with both FR and organoclay, had a lower peak heat release rate (PHRR) and average mass loss rate (MLR) than those with only clay or the FR agents. Extended X-ray absorption fine structure (EXAFS) data confirmed that no FR/clay interactions occurred in the solid phase, and that the synergistic effects were due to gas phase reactions. Since this mechanism is not specific, it opens the possibility of formulating self-extinguishing materials from a large class of polymers.

© 2006 Elsevier Ltd. All rights reserved.

Keywords: PMMA; Self-extinguishing; Nanocomposites; Flame retardant

1. Introduction

Very few polymers are naturally self-extinguishing, and most ignite quite easily when exposed to a flame. In particular acrylates, which are commonly used for molded or extruded sheets, paints and shellacs, are highly combustible and very difficult to render flame retardant, even with the addition of large amounts of conventional flame retardant (FR) agents, such as halogenated compounds, phosphorus and inorganic materials. Recently several groups [1–4] have reported that the addition of a small amount of organoclay can significantly decrease the heat release and mass loss rates, as measured by

cone calorimetry. Unfortunately, the same compositions perform poorly when tested by the industrially significant Underwriters Laboratory test UL 94 standard with respect to extinction time. In these cases, it is believed that the excess quaternary ammonium surfactants used to disperse the clays, also increase the probability of early ignition. In addition, even the surfactants that are bound to the clay surface are thermally unstable and decompose to form volatile vapors. The clay which remains is no longer exfoliated or intercalated. Further, a major limitation of the nano-clays is that they only work in the “condensed phase” (i.e. the solid or molten polymer itself) and do nothing to inhibit the flame in the vapor phase. Hence, to date, no “stand-alone” flame retardant composition based on organoclays has been revealed.

A little known property of clays, namely their localization at polymer interfaces, has recently been shown to increase

* Corresponding author. Tel.: +1 631 6328483; fax: +1 631 6325764.

E-mail address: mrafailovich@notes.cc.sunysb.edu (M.H. Rafailovich).

compatibilization of polymer blends which were mechanically mixed in a twin screw extruder [5–10]. Most flame retardant formulas are basically organic molecules with halogen or phosphorus groups and they are not well dispersed in most polymers. We therefore postulated that the synergy reported recently [2] between clays and flame retardant formulations in PP-g-MA may be a more general phenomena which enhances dispersion and hence the efficacy of the flame retardant within the material.

In order to probe this hypothesis, we chose to apply it to the extreme case of (methyl methacrylate) (PMMA), a highly combustible polymer. A common component of many flame retardant formulations is decabromodiphenyl ether (DB), which decomposes at a high temperature and forms hydrogen bromide that quench the radical chain reactions of combustions and the fire spreading process [11]. When heated PMMA is known to unzip rapidly and decompose, without even forming a char, the flame retardant formulation is hard to achieve. Here, we show that through the addition of standard amounts of FR agents, decabromodiphenyl ether (DB) and antimony trioxide (AO) in combination with clays, even PMMA can pass the stringent UL 94 V0 certification. We further propose a model for this synergy based on transmission electron microscopy of serial sections that were burned for different times, pyrolysis gas chromatography/mass spectrometry (Py-GC–MS) to measure the rate of halogen gas release, and extended X-ray absorption fine structure (EXAFS) to determine the chemical nature of the interactions with the halogen materials.

2. Experimental section

2.1. Materials

Poly(methyl methacrylate) was purchased from Sigma Aldrich with average molecular weight of 120 K. Cloisite 20A was provided by Southern Clay Products Inc., which is a natural montmorillonite modified with *N,N*-dimethyl dihydrogenated tallow quaternary ammonium chloride. Decabromodiphenyl ether was also from Sigma Aldrich with purity >98%. Antimony trioxide was provided by Great Lake Chemical Corporation.

2.2. Sample preparation

The materials were prepared by melt mixing a total of 50 g, at 170 °C in a Brabender. The material was first divided into different weight ratios of PMMA, decabromodiphenyl ether (DB), antimony trioxide (AO), or Cloisite 20A. In order to obtain thorough mixing, the PMMA polymer was first inserted into the chamber and mixed at 20 rpm for 2 min. The clay, DB and AO were then added, once the PMMA was molten, and mixed at 100 rpm for 15 min. While mixing, nitrogen was purged through the chamber to dissipate the additional heat created by the high shear and to avoid the sample degradation. The samples were then pelletized and molded by a hot press into different shapes required for the various characterization techniques described below. The integrity of

the PMMA polymer after mixing at 170 °C was checked using FTIR, and no observable degradation could be found.

2.3. Characterization

Cross sections of the molded materials were obtained by slicing the sample into thin films (around 70 nm thick) at room temperature, using a Reichert-Jung Ultracut E microtome with a diamond knife. The ultra-thin films were then floated from water onto copper grids. Then morphology of the sample was observed using a JEOL JEM1200ex transmission electron microscope (TEM) at 80 kV.

The flame retardant characteristics of the PMMA/clay nanocomposites were tested using a cone calorimeter at the National Institute of Standards and Technology, with a heat flux of 50 kW/m² using a cone radiator. The heat release rate (HRR), as well as the mass loss rate (MLR), was recorded as a function of time. Samples were prepared by compression molding (around 30 g) in 7 cm by 7 cm by 3 mm (thick) square stainless steel molds with a hot press.

UL 94 vertical burning test is a method used in industry to evaluate the fire retardance of the materials, which tests the ease of the ignition of polymeric materials using small burner. Standard bar specimens of PMMA composites (125 mm long by 13 mm wide, 5 mm thick) were molded by a hot press at 170 °C for the UL 94 V0 20 mm vertical burning test. Five specimens were preconditioned with 50% relative humidity for 48 h at 25 °C, and other five specimens were preconditioned in air circulating at 70 °C for 168 h. All of 10 samples were then tested in accordance with ASTM D 3801 UL 94 V0 standard at the Melville Division of Underwrites Laboratories Inc. The results reported are the average of 10 samples for each type of material. Thermogravimetric analysis (TGA) was conducted using a Perkin Elmer TGA7 under air flow, in a heating range from room temperature to 800 °C at a rate of 20 °C/min.

The limiting oxygen index (LOI) was measured by FTA 710 oxygen analyzer from Stanton Redcroft according to ASTM D 2863. Standard bar samples (100 mm long by 6 mm wide, 3 mm thick) were prepared by a hot press and then put into the sample holder inside the chimney for the measurements. The LOI value was defined as the minimum oxygen concentration to support 180 s or 50 mm length burning.

The ion time-of-flight secondary ion mass spectroscopy (ToF-IV SIMS) was equipped with a liquid metal source (Ga) three-lens analyzing gun. The incidence angle of the beam was 45°. The analyzing gun uses isotopically enriched ⁶⁹Ga with less than 0.1% ⁷¹Ga and was pulsed with a 100 ms cycle time and a 100 ns pulse width. The Ga⁺ ion energy and average current were 25 keV and 1 pA, respectively. The Ga⁺ beam was rastered over an area of 50 × 50 μm² with 256 × 256 points. The charging of the polymer samples was neutralized by using a pulsed low-energy electron flood gun (20 eV, 5 μA current) in between analytical pulses. The negative secondary ion (SI) intensity in the mass range of 1–250 Da was measured for each point of the 256 × 256 raster. The lateral resolution was better than 0.5 μm. To enhance the image contrast, 10 scans were

combined. The color scale of the SI intensity was adjusted for each image separately to give best possible representation of the SI images and does not indicate absolute SI intensity.

The samples for extended X-ray absorption fine structure (EXAFS) measurements consisted of the reference DB, PMMA/DB/AO, PMMA/DB/AO burned for 10 s, PMMA/DB/AO/clay, PMMA/PMMA/DB/AO/clay burned for 10 s. The Br K-edge XAFS data were measured in all samples in transmission mode, using the X11B beamline at the National Synchrotron Light Source, Brookhaven National Laboratory. As X-ray detectors, we used ionization chambers filled with the Ar:N₂ (1:2) mixture for incident beam and pure Ar for transmitted beam intensity measurements. The Si (111) double crystal monochromator, 30% detuned to minimize harmonics, was used to scan X-ray energy from 150 eV below the Br K-edge (13,474 eV) to 1000 eV above it. Four scans were averaged for each sample. The data were processed with the IFEFFIT package [12]. After removing the smooth background function from the X-ray absorption coefficient, and normalizing by the edge jump, the thus-obtained $\chi(k)$ data were k^2 -weighted and Fourier transformed to k -space. Due to the noise at high k in the burned sample data, the k -range for Fourier transforms was between 2 and 8 Å⁻¹.

About 6 mg of sample was heated from ambient temperature to the desired temperature 600 °C with a heating rate of 30 °C/min. Then the sample was pyrolyzed at 600 °C for 20 s. The analyses were conducted on PYRAN (a thermal degradation unit from ThermEx) combined with an HP gas chromatography/mass spectrometry (GC–MS) engine. Volatiles were trapped by liquid nitrogen at –60 °C during the thermal degradation process. At the end of the thermal degradation, volatiles were released into gas chromatography/mass spectrometry (GC–MS) for analysis. GC oven was heated from 30 to 300 °C at 10 °C/min. Mass range was set at 30–650 Da.

3. Results and discussion

3.1. Morphological characterization

In Fig. 1 we show the TEM images from thin cross sectional slices obtained from PMMA/DB/AO (70/20/5) samples

with and without 5% Cloisite 20A clay. From the figure we can see that the DB and AO (dark areas with larger electron densities) are dispersed into the PMMA polymer. In the absence of clay, large domains, several microns in diameter, are clearly visible. In Fig. 1b, we show the TEM cross section of the sample with the same composition, but with 5% Cloisite 20A clay. The inset is a high resolution image of the same sample with an expanded scale. From the figure we see that the clay is well intercalated or exfoliated in the PMMA matrix and the clay platelets are oriented along the shear direction. The only exceptions are the clay platelets at the DB/AO/polymer interfaces, which orient themselves along the curved interphase boundaries, rather than along the shear direction. In this case, most of the particles were around 2 nm except a few larger aggregates.

Fig. 2a and b represents time-of-flight (TOF) secondary ion mass spectrometry (SIMS) images of the same PMMA/DB/AO (70/20/5) composites with and without clay, respectively. In this case we have chemical specificity and can directly measure distribution of individual species within the sample, since the SIMS technique can be made to raster the surface with a window placed to identify different masses. In Fig. 2, we show TOF-SIMS data obtained from the same samples, where we placed a digital window on the mass of the Br ion. From Fig. 2a, we can see that large domains of Br are present in the sample, where we assume that DB is located. In the sample where clay was added, Fig. 2b, we see many more, albeit smaller domains, with less Br in each, scattered over a wider area of the sample. These data are in agreement with the TEM micrographs and here too we can clearly see that the dispersion of the Br is far better in the samples with clay.

3.2. Flame retardancy

The PMMA and the PMMA nanocomposites were subjected to the UL94 V0 flame test and the results are summarized in Table 1. In this test, a flame is applied to the sample for 10 s and removed. The time that the sample continues to burn is recorded as t_1 . The flame is then reapplied a second time for 10 s and the burning time after removal is recorded as t_2 . In addition, a piece of cotton is placed under

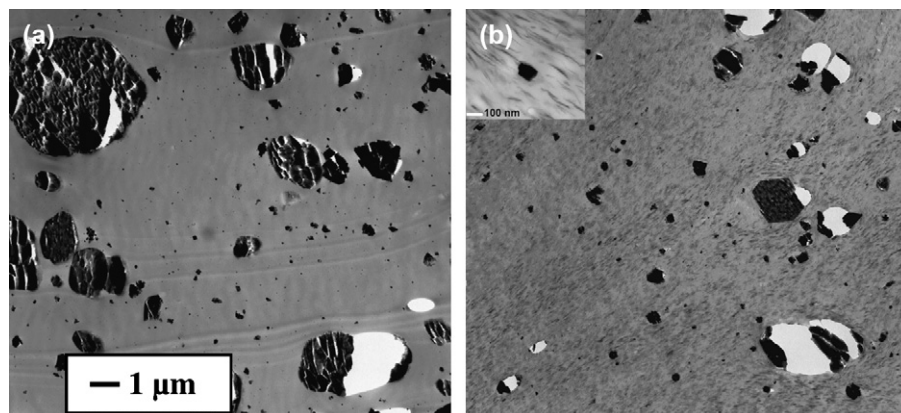


Fig. 1. TEM images of PMMA composites: (a) PMMA/DB/AO (75/20/5) and (b) PMMA/DB/AO/Cloisite 20A (70/20/5/5).

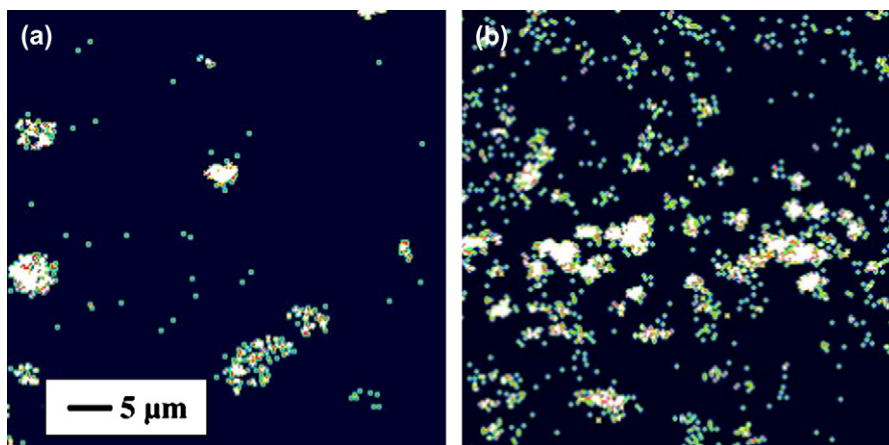


Fig. 2. 50 $\mu\text{m} \times 50 \mu\text{m}$ Secondary images (SI) of PMMA composites (M79: Br⁻): (a) PMMA/DB/AO (75/20/5) and (b) PMMA/DB/AO/Cloisite 20A (70/20/5/5).

the sample, which will ignite if the sample has flaming drips during burning. In order to pass this test, the cotton must not ignite and the sum, $t = t_1 + t_2$, must be less than 10 s. The pure PMMA continued to burn till the sample was entirely consumed after the first application of the flame. Furthermore, it also dripped vigorously and ignited the cotton. Addition of the FR formulation of DB and AO, the composite self-extinguished within 16 s after the first application of the flame, without dripping. After the second application, the sample could not self-extinguish and continued to burn and drip, indicating that the internal composition had changed. The sample where both FR and only 5% clay were added self-extinguished in 1 s after the first application of the flame without dripping. The behavior was identical after the second application of the flame, indicating that the composition of the material had not changed. Even though this was sufficient to obtain UL 94 V0 certification, we repeated the burning cycle for at least another five times with identical results, indicating that the composite was completely stable against this type of ignition. Optical images of the samples are shown in Fig. 3, where we can see that the PMMA sample containing both FR and clay is blackened by the smoke of the flame, but unchanged in shape.

It should be noted that dripping was suppressed in all samples containing clays, whether or not they contained the FR formulation. In Fig. 4, we show the modulus of the samples as a function of temperature, as obtained from DMA analysis. From the figure, we can see that the modulus increases by more than 100% for $T > T_g$, hence the increased viscosity decreases the tendency to drip.

Table 1
UL 94 V0 test results and LOI values of PMMA and PMMA composites

Materials	UL 94 V0	LOI (%)
PMMA	Dripping and burning (failed)	16.9
PMMA/DB/AO (75/20/5)	Dripping and burning ($t_1 = 16$ s failed)	23.3
PMMA/DB/AO/Cloisite 20A (70/20/5/5)	Passed ($t_1 = 1$ s, $t_2 = 1$ s)	25.6

The burning process of a material is best characterized using cone calorimetry [11]. This technique can provide the heat release rate (HRR), the mass loss rate (MLR) as well as the ignition time in small-scale fires (normally heat flux is 35 or 50 kW/m^2), which provides information as to the internal chemistry during burning. Fig. 5 shows the HRR and MLR curves of pure PMMA and the composites. The exact values are tabulated in Table 2. From the figure and the table we can see that all three materials have approximately the same ignition time. The PMMA and PMMA/FR/clay ignite in 22 s, while the PMMA/clay ignites slightly sooner, in 20 s, due to the excess surfactant, which is known to ignite easily [2]. From the figure it is also clear that pure PMMA burns

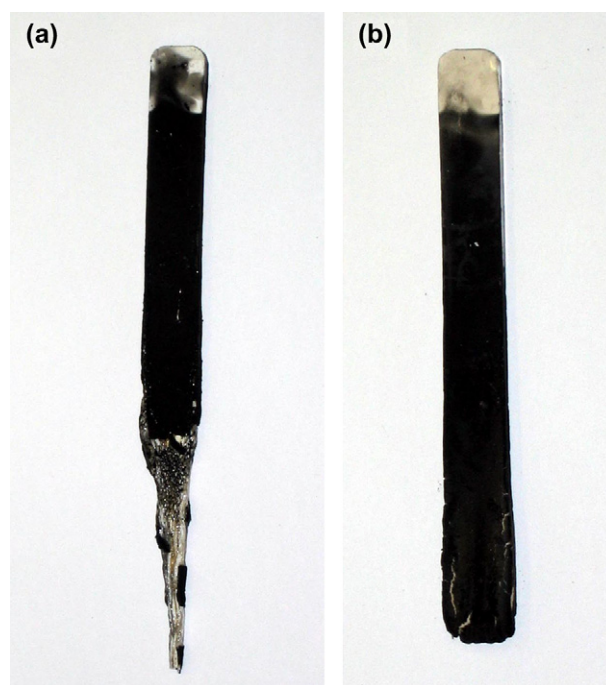


Fig. 3. Optical images of PMMA composites after the combustion of UL 94 V0 test: (a) PMMA/DB/AO (75/20/5) and (b) PMMA/DB/AO/Cloisite 20A (70/20/5/5).

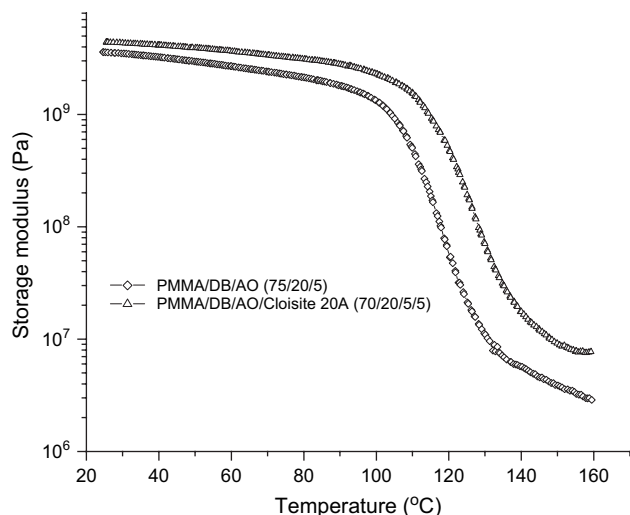


Fig. 4. Storage modulus as a function of temperature of PMMA/DB/AO (75/20/5) and PMMA/DB/AO/Cloisite 20A (70/20/5/5).

intensely, with a well defined peak heat release rate (PHRR) of 1500 kW/m², which is now widely accepted to represent the maximum intensity of fire by this material [13]. From the figure we can also see that the addition of the FR decreased the PHRR by more than a factor of 3 to less than 490 kW/m² and the average HRR by 65.2% to nearly 306 kW/m². Addition of 5% clay further decreases the PHRR to 359 kW/m² and the average HRR by 48.7%. Addition of either clay or FR produces a uniform HRR and hence eliminates the PHRR. The heat release rate of PMMA/clay composite with DB and AO increased more quickly than pure PMMA and the system with only DB and AO before 40 s. That is believed to be due to the thermal decomposition of organic surfactant in the clay layers, which were converted to volatile components. Yet, despite the slightly larger heat release in the early stages of combustion, the PMMA/DB and AO/clay composite exhibited the longest burning time and the highest fire performance index of the three compounds (Table 2).

The addition of DB, AO and clay also has large effect on decreasing the mass loss rate, as shown in Fig. 5b. It is interesting to note though, that in the early stages of combustion, $t < 100$ s, the pure PMMA had the lowest mass loss rate. The largest initial MLR was for the sample with clay, where again the MLR could be attributed to the excess unbound surfactant or its breakdown products, which are known to be volatile. The slightly larger MLR of the composite containing only the FR formula could be attributed to the volatility of the DB compound. For $t > 100$ s, the pure PMMA exhibits a sharp peak in the MLR, due to unzipping of the PMMA chains and rapid evaporation of the residue. The addition of FR formulation damps this phenomenon and decreases the MLR. Addition of clay further enhances this effect and decreases the MLR by nearly a factor of 2 for $t > 200$ s.

The limiting oxygen index (LOI) values of pure PMMA and PMMA composites are shown in Table 1. The low LOI value (16.9) of pure PMMA reflects its high flammability. The combination of DB and AO increased the LOI value of

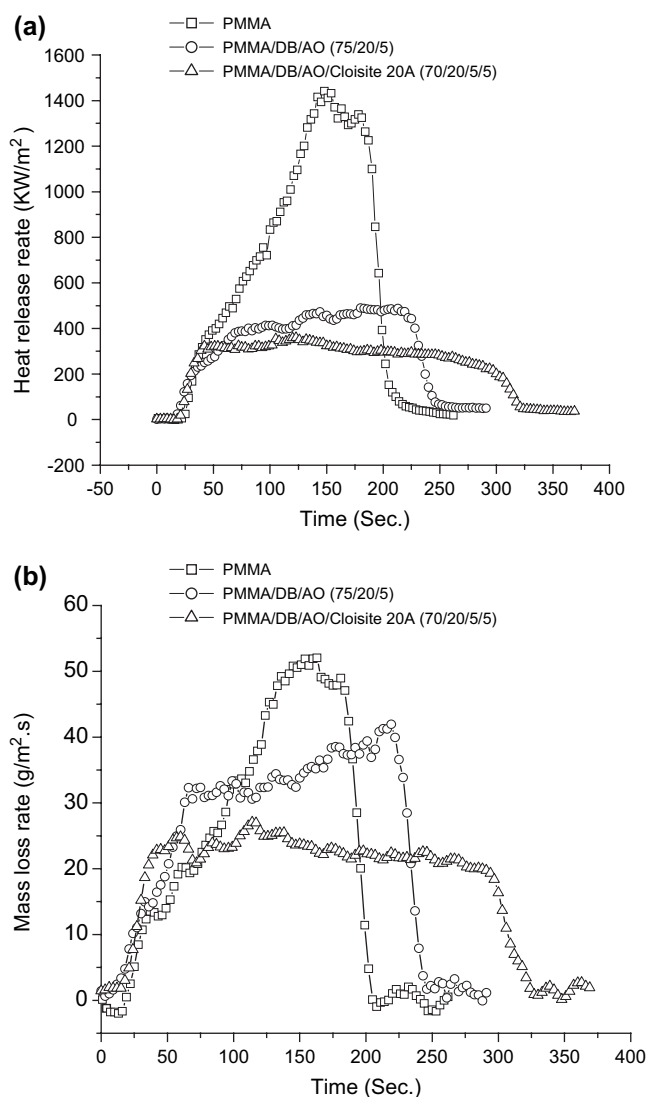


Fig. 5. Heat release rate curves (a) and mass loss rate curves (b) of PMMA and PMMA composites.

PMMA to 23.3. The addition of 5% Cloisite 20A further increased the LOI to 25.6, which is low, but just within the acceptable range of 24 and higher, which is known for other materials that have obtained a UL 94 V0 rating [13].

From these data it is clear that a favorable combined synergy exists as a result of having the clay and the FR components both present. The following questions can then be asked; first, does the clay, which is known to be a gas

Table 2
Cone calorimetry test data of PMMA and PMMA composites

Sample	Peak HRR (kW/m ²)	Average HRR (kW/m ²)	Average MLR (g/s)	Fire performance index (10 ⁻³ s m ² /kW)
PMMA	1456.8	598.5	0.138	18
PMMA/DB/AO (75/20/5)	490.4	306.9	0.177	45
PMMA/DB/AO/Cloisite 20A (70/20/5/5)	359.4	235.9	0.125	56

permeability barrier, hinder the vapors of DB from escaping from the composite and hence make it more effective in reacting with the gas phase of the polymer? Or second, is it simply the fact that the DB is better dispersed in the matrix and hence the particles come in better contact with the polymer and can vaporize more easily since the average diameters are much smaller? Or finally, is it possible that the clay may be a catalyst which facilitates the gas phase reaction of the DB? Or the reaction of the DB and with the antimony trioxide?

3.3. Structure evolution during combustion

To further investigate how the structure of the clay and the FR components changed during combustion, different samples of the composite were burned according to UL 94 V0 standard by exposure to the flame for different times, increasing in steps of 3 s. Thin sections were then microtomed from the area where the samples were directly exposed to the flame. Fig. 6a–d shows the TEM images of PMMA/DB/AO/Cloisite 20A (70/20/5/5) sections from samples that were burned for 0 to 3, 6, and 9 s. From Fig. 6a, we can see that prior to burning, the FR is dispersed in particles ranging from 200 nm to several tens of nm in size. The clay platelets are also well dispersed with a combination of tactoidal, intercalated and exfoliated regions. No specific orientation is visible. From Fig. 6b,

we find that after only 3 s of burning the clay platelets become aligned parallel to the vertical direction i.e. in the directions where the molten material is stretched by gravity. The clay platelets are also observed to self-assemble into larger aggregates and many of the smaller FR particles have disappeared. A similar aggregation was also observed previously in PMMA/clay composites without FR [14] where it was shown that this was a result of the surfactant desorbing from the clay platelet surfaces, for $T > 250$ °C, and evaporating. The highly charged surfaces of the platelets were no longer screened and they reassembled into tactoidal structures. The process continued further after burning for 9 s, where we can see the clay platelets continued to self-assemble into ordered rope-like structures composed mostly of intercalated tactoids. These structures may be responsible for what appears like a surface char layer on the samples which, as suggested by Gilman et al. [3], may be responsible from shielding the underlying material from the burning process and decreasing the mass loss rate of the decomposing products. The mean particle size continued to decrease and the very small particles, whose diameters were less than 10 nm, completely disappeared, indicating that the self-extinguishing properties were somewhat related to the vaporization of the FR components.

The samples were also examined using EXAFS at the BNL/NSLS facility. The data are shown in Fig. 7, where the Fourier

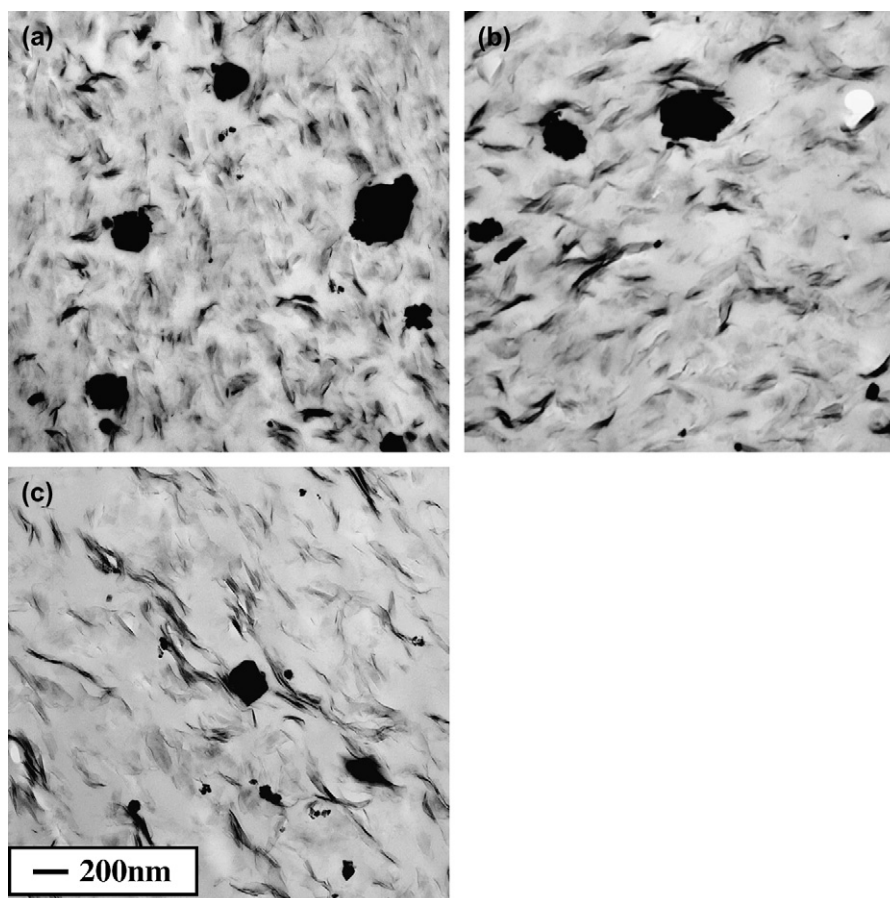


Fig. 6. Structure evolution TEM images of PMMA/DB/AO/Cloisite 20A (70/20/5/5) burned for different time: (a) 0 s, (b) 3 s, and (c) 9 s.

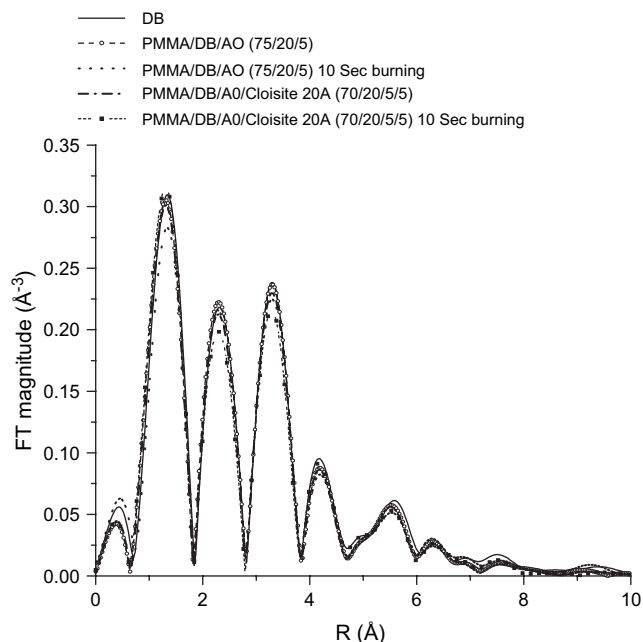


Fig. 7. Fourier transformed magnitude of k^2 -weighted EXAFS data of the reference DB and PMMA composites.

transformed magnitudes of the absorption coefficients in background-subtracted are plotted. The peaks in the spectra are caused by the presence of nearest neighbors, and their positions and intensities are directly related to the chemistry and geometry of the local surrounding of the Br absorbing atom. From the figure we see that the spectra are nearly identical for all samples. This indicated that the Br retained the same chemical environment that it originally had in the DB even after mixing with PMMA, PMMA/clay and burning for as long as 10 s. Hence, we can conclude that no reactions with the Br occur in the solid phase to produce new kinds of Br structures which stay in the condense phase and the flame retardant properties must originate in the gas phase chemistry.

3.4. Effect of clay on the vapor phase

It has been demonstrated that pyrolysis GC–MS is suitable for the analysis of brominated organic products from flame retarded polymers under thermal decomposition [15]. We, therefore, heated the samples to 600 °C for 20 s and the pyrograms of PMMA/DB/AO/(75/20/5) nanocomposite with and without 5% Cloisite 20A clay are shown in Fig. 8. For convenience, the intensity of all the products was normalized to MMA (100%) and the data are listed in Table 3. Here we find large differences produced by the addition of the clay. The amplitudes of the peaks corresponding to decomposition of only the PMMA are similar between the two spectra. On the other hand, large increases in the amplitude of peaks 7 and 9 and a decrease in the amplitude of peaks 8 and 10 is observed. This indicates that the clay somehow affects the reaction mechanisms in the gas phase.

From the table we can clearly see that the intensity of peak 9 of the sample plus the clay is significantly higher than that of the sample without clay, which belongs to 3,6-dibromo-5,8-dihydroxy-2-methyl-1,4-naphthalenedione. This compound may be derived from a segment by cyclization and strong debromination of the decabromodiphenyl ether. Similar mechanism might produce the segments as well as peaks 7, 8 and 10. Since the clay is not volatile and does not react with the DB directly, we can only surmise that the clay somehow has a catalytic function, similar to the AO, which enhances the reactions between the DB and the MMA gases. This effect, combined with the improved dispersion and possible confinement of the vapors may explain the synergy observed. Recent data [16] have shown that this effect can occur in many other homopolymers and blends, and hence is a somewhat general phenomenon.

4. Conclusion

Self-extinguishing PMMA composites, which can pass the stringent UL 94 V0 standard, can be successfully prepared by

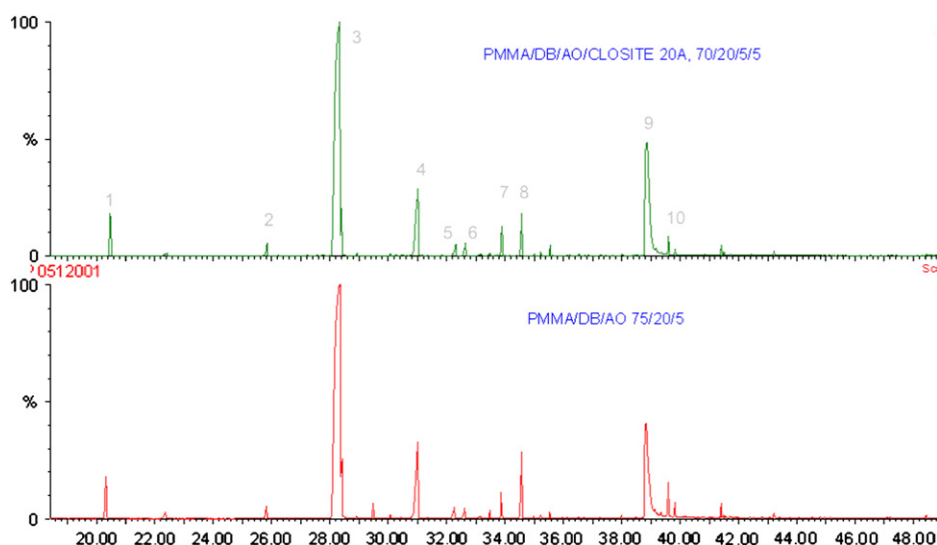


Fig. 8. Pyrograms of PMMA/DB/AO/Cloisite 20A (70/20/5/5) and PMMA/DB/AO (75/20/5) heated for 20 s at 600 °C.

Table 3
Identities and comparison of the released gases of thermal decomposition of flame retardant composites as determined by pyrolysis GC–MS

Peak no.	Retention time (min)	No clay	With clay	Peak ID
1	20.34	4.5	5.5	Methane, bromo-
2	25.83	1.2	1.3	2-Propenoic acid, methyl ester
3	28.32	100.0	100.0	MMA
4	31.02	13.2	15.0	Methyl 2-methoxypropenoate
5	32.27	1.3	1.7	2,5-Furandione, 3-methyl-
6	32.61	1.1	1.5	2-Butenoic acid, 4-hydroxy-, methyl ester
7	33.88	1.5	2.3	Methyl 2-(bromomethyl)acrylate
8	34.58	5.8	3.8	2,3-Butanediol, 1,4-dibromo-2,3-dimethyl-
9	38.83	28.9	43.0	3,6-Dibromo-5,8-dihydroxy-2-methyl-1,4-naphthalenedione
10	39.60	2.2	1.4	Brominated 2-cyclopentene-1,2-dicarboxylic acid, 3-methyl-, dimethyl ester

combining modified clays with traditional flame retardant (FR) agents, DB and AO. The addition of clay effectively improves the dispersion of the FR agents and increases the viscosity of the polymer which helps maintain the shape of the sample during burning. The nanocomposites with all three components, clay, DB and AO show a lower PHRR and average MLR than those with only clay or the FR agents. EXAFS data confirm that the FR formulation does not react in the solid phase. TEM and pyrolysis GC–MS measurements of serially burned samples indicate that the clay plays various roles on quenching the flame, such as promoting the char formation, increasing the dispersion of the FR, and catalyzing the chain reaction. The synergism between clay and conventional FR agents provides an alternative for improving fire performance. Since this mechanism is not specific to PMMA, it opens the possibility of formulating self-extinguishing materials from a large class of polymers.

Acknowledgements

Partial support for this work was obtained from the NSF-MRSEC program. We acknowledge the support by the US Department of Energy Grant No. DE-FG02-03ER15477.

References

- [1] Alexandre M, Dubois P. *Mater Sci Eng* 2000;28:1.
- [2] Zanetti M, Camino G, Canavese D, Morgan AB, Lamelas FG, Wilkie CA. *Chem Mater* 2002;14:189.
- [3] Gilman JW, Jackson CL, Morgan AB, Harris Jr R. *Chem Mater* 2000;12:1866.
- [4] Hu Y, Wang S, Ling Z, Zhuang Y, Chen Z, Fan W. *Macromol Mater Eng* 2003;288:272.
- [5] Zhu S, Liu Y, Rafailovich M, Sokolov J, Gersappe D, Winesett DA, et al. *Abstra Pap ACS* 1999;218:109.
- [6] Petridis D, Voulgaris D. *Polymer* 2002;43:2213.
- [7] Gelfer MY, Song HH, Liu L, Hsiao BS, Chu B, Rafailovich M, et al. *Polym Sci Part B Polym Phys* 2003;41:44.
- [8] Yurekli K, Karim A, Amis EJ, Krishnamoorti R. *Macromolecules* 2003;36:7256.
- [9] Wang Y, Zhang Q, Fu Q. *Macromol Rapid Commun* 2003;24:231.
- [10] Si M, Arkai T, Zou Y, Ade H, Kilcoyne ALD, Fisher R, et al. *Macromolecules* 2006;39:4793.
- [11] Grand AE, Wilkie CA. *Fire retardancy of polymeric materials*. Marcel Dekker, Inc.; 2000.
- [12] Newville MJ. *Synchrotron Rad* 2001;8:322.
- [13] Weil ED, Hirschler MM, Patel NG, Shaki S. *Fire Mater* 1992;16:159.
- [14] Si M, Goldman M, Rudomen G, Gelfer M, Sokolov J, Rafailovich M. *Macromol Mater Eng* 2006;6:602.
- [15] Jakab E, Uddin MA, Bhaskar T, Sakata YJ. *Anal Appl Pyrolysis* 2003;68:83.
- [16] Si M., et al. *MRS meeting*; 2005, Fall.